You, R., Lin, C.-H., Wei, D., and Chen, Q. 2019. "Evaluating the commercial airliner cabin environment with different air distribution systems," *Indoor Air*, □□

Evaluating the Commercial Airliner Cabin Environment with Different Air Distribution Systems

Ruoyu You[1,2], Chao-Hsin Lin[3], Daniel Wei[4], and Qingyan Chen[2*]

[1] Department of Building Services Engineering, The Hong Kong Polytechnic University, Hong Kong SAR, China
[2] School of Mechanical Engineering, Purdue University, West Lafayette, IN 47907, USA
[3] Environmental Control Systems, Boeing Commercial Airplanes, Everett, WA 98203, USA
[4] Boeing Research & Technology, Beijing 100027, China
[*] Phone: (765) 496-7562, Fax: (765) 496-0539, Email: yanchen@purdue.edu

Abstract

Ventilation systems for commercial airliner cabins are important in reducing contaminant transport and maintaining thermal comfort. To evaluate the performance of a personalized displacement ventilation system, a conventional displacement ventilation system, and a mixing ventilation system, this study first used the Wells-Riley equation integrated with CFD to obtain the SARS quanta value based on a specific SARS outbreak on a flight. This investigation then compared the three ventilation systems in a seven-row section of a fully occupied, economy-class cabin in Boeing 737 and Boeing 767 airplanes. The SARS quanta generation rate obtained for the index patient could be used in future studies. For all the assumed source locations, the passengers' infection risk by air in the two planes was the highest with the mixing ventilation system, while the conventional displacement ventilation system produced the lowest risk. The personalized ventilation system performed the best in maintaining cabin thermal comfort and can also reduce the infection risk. This system is recommended for airplane cabins.

Keywords: Computational fluid dynamics (CFD); Personalized ventilation; Displacement ventilation; Mixing ventilation; Infectious disease transmission; Thermal comfort.

Practical Implication:

Air distribution plays a critical role in creating a healthy and thermally comfortable environment in airplane cabins. This investigation evaluated the performance of three ventilation systems in terms of SARS infection risk by air and thermal comfort in a single-aisle commercial airliner and a twin-aisle airliner. The three systems were mixing ventilation, conventional displacement ventilation, and personalized displacement ventilation. The results could be used in the design of air distribution systems for a better cabin environment.

1. Introduction

The transmission of airborne infectious diseases, including influenza[1], tuberculosis[2], and severe acute respiratory syndrome (SARS)[3], has been observed in commercial airliners. As the number of air passengers[4] increases, attention has been drawn to creating a cleaner and healthier cabin environment. Air distribution is critical in controlling contaminant transport[5-8] and maintaining thermal comfort[9-12] in aircraft cabins. Therefore, it is necessary to investigate the use of different air distribution systems to improve the cabin environment.

Currently, mixing ventilation systems are prevalently installed in commercial airliners to provide an acceptable cabin environment. A mixing ventilation system supplies clean air through diffusers in the ceiling and/or at shoulder level, and extracts the cabin air through exhaust slots in the side walls near the floor. In most commercial airliner cabins, a system of gaspers is also installed to provide supplementary personalized ventilation. The gaspers are small circular vents above the seats, one for each passenger. They provide clean air as an additional means of regulating thermal comfort and are adjustable for both flow rate and direction.

For investigation of the air distribution in aircraft cabins, laboratory tests have been carried out in small cabin mockups to characterize the jets along the diffusers[13], the main flow in the cabin[14-16], thermal plumes from heated manikins[17], and gasper-induced flow[18-21]. At the same time, efforts have been made to evaluate contaminant transport in cabins. For instance, Zhang et al.[22] measured the air velocity, temperature, and gaseous and particulate contaminant concentrations in a section of a half-occupied, twin-aisle cabin mockup with a mixing ventilation system. They found that contaminant concentration in the four-row cabin was fairly uniform, indicating that mixing ventilation was not efficient in controlling contaminant transport. Li et al.[23] measured the distributions of air velocity, temperature, and contaminant concentration by using the tracer gas SF_6 in a five-row section of the economy cabin of an MD-82 airplane with the gaspers turned on. The results showed that even though the gasper system had an impact on the air velocity and contaminant transport in the cabin, it might not improve cabin air quality. The above experimental studies have indicated that the current air distribution systems in airliner cabins are not efficient in controlling the transport of airborne infectious diseases.

In addition to experimental studies, computational fluid dynamics (CFD) has been used extensively in the cabin environment, to design and optimize air supply [24-28], predict transient particle transport[29-31], evaluate airborne infectious diseases risks[32-34], and identify source location[35,36]. For example, Qian et al.[32] combined the CFD simulations and Wells-Riley equation to evaluate the spatial distribution of infection risk of SARS transmission in a hospital ward. Yan et al.[33] used a Lagrangian-based Wells-Riley approach to evaluate the airborne disease infection risks in an airliner cabin. Studies have also focused on the performance of existing air distributions in contaminant control in commercial airliners. For instance, Zhang and Chen[37] calculated the distributions of the air velocity, air temperature, and CO_2 concentration in a section of a Boeing 767 aircraft cabin with a mixing ventilation

system. They found that the system could spread infectious diseases, since the CO_2 concentration distribution was fairly uniform. You et al.[38,39] developed a simplified gasper geometry and a consolidated turbulence model for use in a CFD software program to predict the airflow and contaminant transport in an airliner cabin with gaspers. The CFD program was used to investigate the impact of gaspers on cabin air quality in the economy-class cabin of Boeing 767 and Boeing 737 airplanes. The results showed that, even though the gaspers provided clean air, the statistical impact of the gaspers on passengers' exposure to contaminants was neutral.

To effectively control airborne contaminant transport in an aircraft cabin, new ventilation systems should be developed. Bosbach et al.[40] compared the air velocity and temperature distributions in an A320 cabin with mixing ventilation and conventional displacement ventilation during flight tests. They found that the mixing ventilation system had a low heat-removal efficiency, indicating that the system might not be efficient in controlling contaminant transport if contaminant sources were associated with heat sources. Schmidt et al.[41] and Müller et al.[42] compared mixing and conventional displacement ventilation systems in a section of an A320 cabin mockup. Schmidt et al.[41] found that the displacement ventilation system produced "hot heads," while the mixing ventilation system presented a higher draft risk. On the other hand, Müller et al.[42] suggested that the displacement ventilation system could maintain an acceptable cabin thermal environment as long as the temperature difference between the head and feet was sufficiently small. To improve the contaminant transport efficiency while maintaining thermal comfort in a cabin, we[43] previously proposed a personalized displacement ventilation system. In this system, individual diffusers were installed in the floor under the seat to supply fresh air directly to passengers in the row behind, and the cabin air was exhausted at ceiling level. We measured the air and temperature distributions in a seven-row cabin mockup with the personalized displacement ventilation system, and found that the system provided acceptable air distributions. We then used CFD to assess the system in terms of contaminant removal efficiency in a one-row cabin. However, the removal efficiency might not fully characterize the longitudinal contaminant transport, and thus further efforts should be made to systematically investigate the contaminant transport between rows in an aircraft cabin when the proposed ventilation system is used.

To evaluate the performance of mixing ventilation, conventional displacement ventilation, and personalized displacement ventilation systems, this study first used the Wells-Riley equation integrated with CFD to obtain the SARS quanta value based on an outbreak on a flight from Hong Kong to Beijing during the 2003 SARS epidemic. This investigation then calculated the SARS infection risk by air and risk of draft in a seven-row section of the fully occupied, economy-class cabin of two commercial airplanes, Boeing 737 and Boeing 767, with the three ventilation systems. The results were then used to evaluate the performance of the systems in controlling contaminant transport and maintaining cabin thermal comfort.

2 Method

In the literature review above, we also found that experimental investigation of airflow and contaminant transport in an airliner cabin is expensive and time consuming, and the reported measurements are not free from errors. Our earlier investigations[26,44] compared CFD results with experimental data in various air distribution studies in airliner cabins. We concluded that CFD can provide informative results with acceptable accuracy. Thus, the present investigation has used CFD, and this section details the CFD method and other models that were needed.

2.1 Airflow, turbulence, and contaminant model

For numerical determination of the air and contaminant distributions in aircraft cabins, it is important to choose an accurate turbulence model. Among all Reynolds-averaged Navier-Stokes (RANS) models, the RNG k-ε model is the most robust in simulating the bulk-airflow regions for enclosed environments[44-47], and the SST k-ω model is superior in the near-wall regions[44]. To take advantage of both models, we[44] proposed a hybrid model that activates the standard k-ω model in the near-wall region and a transformed RNG k-ε model in the bulk-airflow region. The hybrid model uses a blending function to gradually transition between the two models. Considering its advantage in predicting both the bulk-airflow and near-wall regions, the hybrid SST k-ω and RNG k-ε turbulence model was used in this investigation to evaluate the ventilation systems.

To simulate the contaminant transport in an aircraft cabin, this study used the Eulerian method[48]:

$$\frac{\partial \phi}{\partial t}+\frac{\partial}{\partial x_i}\left(\rho \phi U_i\right)=\frac{\partial}{\partial x_j}\left(\Gamma_\phi \frac{\partial \phi}{\partial x_j}\right)+S_\phi \tag{1}$$

where ϕ is contaminant concentration, t is time, x_i is coordinate, ρ is air density, U_i is air velocity, Γ_ϕ the diffusion coefficient, and S_ϕ the mass flow rate of source per unit volume. A detailed description of all terms can be found in ANSYS[49]. The turbulent Schmidt number was set at 1[50].

The hybrid turbulence model and the Eulerian model have been validated by experimental data in our previous study[43]. We manufactured an innovative personalized displacement ventilation system and installed it in a fully occupied, full-scale, single-aisle, cabin mockup. The cabin had seven rows, each with six seats. Heated manikins were used to simulate passengers inside the cabin. The boundary conditions were carefully measured. A constant-injection SF_6 tracer-gas technique was used to measure the flow rate for each diffuser, while an infrared camera was used to measure the surface temperature distribution of the manikins. We used a Particle image velocimetry (PIV) system to obtain the airflow distribution with a

high-resolution in a measuring area of 115 cm wide and 80 cm high. Ultrasonic anemometers were used to further measure the 3D air velocities at 197 sampling points. The air temperature distribution was measured by thermocouples with 426 sampling points. The mixture of 1% SF_6 and 99% N_2 as a tracer gas was injected at the mouth of the manikin seated at 4D and the SF_6 concentration was sampled in front of each passenger and in the middle of the cabin with a total of 41 sampling points using a photoacoustic gas analyzer (INNOVA model 1314). The hybrid turbulence model and Eulerian method were then used to calculate the validation case using the measured boundary conditions. The calculated airflow, temperature, and contaminant distributions were compared with the measured data. The comparison showed that the model was capable of predicting the general trends of the distribution. The detailed information about the validation can be found in You et al.[43].

2.2 Risk assessment

On the basis of the Wells-Riley equation and the calculated contaminant concentration in each passenger's breathing zone, a passenger's infection risk can be estimated as:

$$P_i = 1 - \exp(-C_{q,i} pt) \tag{2}$$

where P_i is the infection risk for the passenger, $C_{q,i}$ the contaminant concentration in the passenger's breathing zone, p the passenger's breathing flow rate, and t the flight duration. Note that the index passenger was assumed to exhale virus continuously during the flight, and the source is set to the quanta of the disease in the CFD calculation.

To determine the SARS quanta value, this study first analyzed a SARS transmission case on a three-hour flight from Hong Kong to Beijing on March 15, 2003[3]. As shown in Figure 1, the index passenger was in seat 14E in the economy cabin of a Boeing 737 airplane. This investigation focused on the SARS transmission due to airborne transport, and a seven-row section of the cabin, from row 11 to row 17, was considered. The total number of infected passengers in the seven-row section was 11, and the overall infection risk was 11/41. Detailed information about this case can be found in Olsen et al.[3]

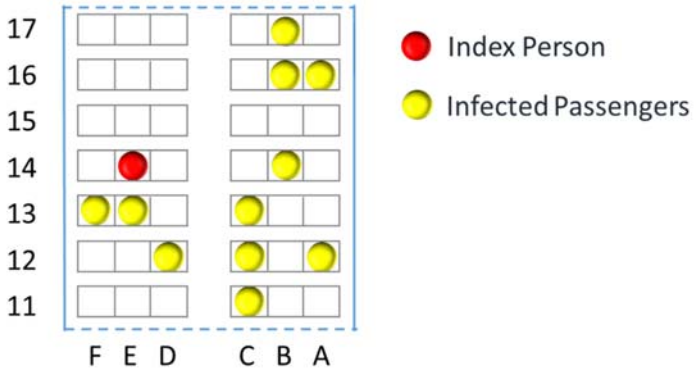

Figure 1. Schematic diagram of a section of the Boeing 737 on a flight from Hong Kong to

Beijing (redrawn from Figure 2 in Olsen et al.[3]).

This study then modeled the contaminant transport in a seven-row section of the fully-occupied, economy cabin of the Boeing 737 to revisit this case. The breathing flow rate of each passenger was set at 0.00053 m^3/s [51]. The source was at the mouth of the passenger in 4E, and the SARS quanta number was obtained by means of the CFD-integrated Wells-Riley equation. With the overall infection risk set at 11/41 and the flight duration at three hours, the SARS quanta number was back-calculated to be 100.8/h. Note that this investigation assumed the airborne route was solely responsible for the SARS infection in the seven-row section of cabin. Thus, this quanta rate was obtained only for the convenience of the cabin section, which might not represent the realistic condition. The obtained value was then used in the following calculations.

2.3 Risk of Draft

To evaluate thermal comfort in an enclosed environment, one would normally use the predicted mean vote (PMV). One could achieve a low PMV value by adjusting the air supply temperature, and thus PMV may not be a meaningful parameter in evaluating different air distribution systems. In the present study, the air supply locations were close to the passengers' feet, which could lead to draft. Therefore, this study focused on the risk of draft and used the predicted percentage of dissatisfied caused by draft (PD) developed by Fanger et al.[52] as a thermal comfort criterion:

$$PD = 3.143(34 - t_a)(\bar{v} - 0.05)^{0.6223} + 0.3696\bar{v}Tu(34 - t_a)(\bar{v} - 0.05)^{0.6223} \quad (3)$$

where t_a is the air temperature, $\bar{v}$ the mean air velocity, and Tu the turbulence intensity. According to ASHRAE standards[53], PD should be less than 15%.

All of the simulations were run under a steady-state condition using the commercial CFD software ANSYS Fluent. User defined functions (UDF) were used to implement the hybrid turbulence model, Eulerian contaminant transport model, Wells-Riley equation, and PD distribution equation.

3. Case Setup

To evaluate the ventilation systems' effectiveness in controlling contaminant transport and maintaining thermal comfort in commercial airliners, we calculated the air distribution, contaminant transport, risk of infection by SARS, and distribution of PD in the economy-class cabins of two popular airplanes, Boeing 737 and Boeing 767, for each of the three systems.

Figure 2 is a schematic of a seven-row section of the fully occupied economy cabin of the

Boeing 737. The ventilation rate and supply air temperature were set at the same values for all three ventilation systems. The mixing ventilation system had two linear air-supply diffusers with a width of 4 mm in the center of the ceiling, labelled as ①, and one diffuser with a width of 20 mm in each wall at shoulder level, shown as ②. The exhausts with a width of 34 mm ③ were located in the lower part of the two side walls near the floor. The personalized displacement ventilation system consisted of individual diffusers uniformly distributed along the floor, one for each passenger, labelled as ④, and ① was utilized as the exhaust. The personalized diffuser opening, with a height and width of the 300 and 80 mm, respectively, was installed under the seat in front of the corresponding passenger. The diffuser grille was designed to direct the flow toward the breathing zone of the passenger. In real applications, the supply air diffusers of the personalized ventilation system can be installed in front of the electrical boxes underneath the seats. Such an installation arrangement can minimize the influence on the passengers' leg room. The conventional displacement ventilation system supplied air through ③, two linear diffusers in the lower side walls, and returned air through the slots in the ceiling, ①. To study the impact of the contaminant's source on its transport, this investigation assumed three source locations at mouth level of the passengers seated at 4D, 4E, and 4F for all three systems. The flight duration was assumed to be two hours.

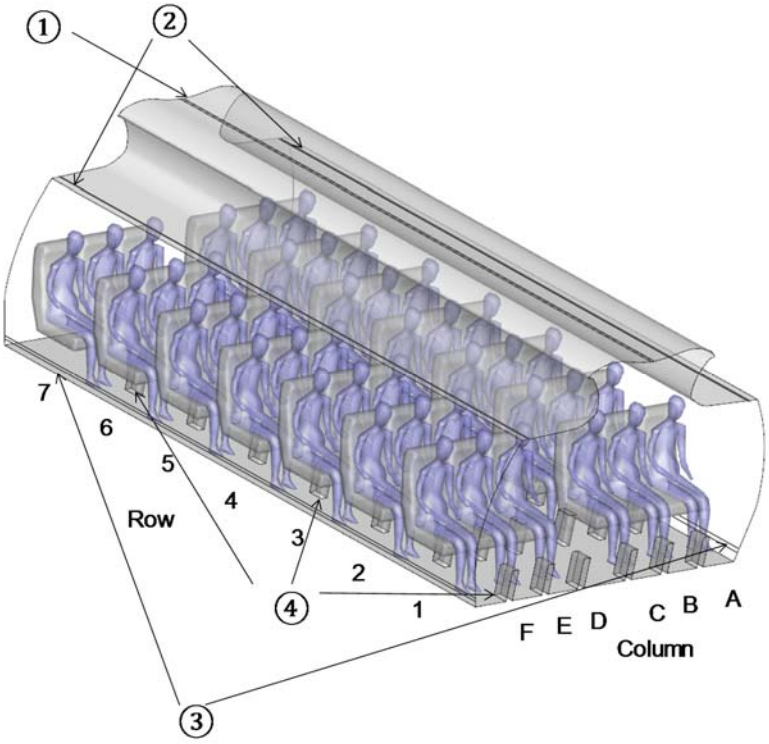

(a)

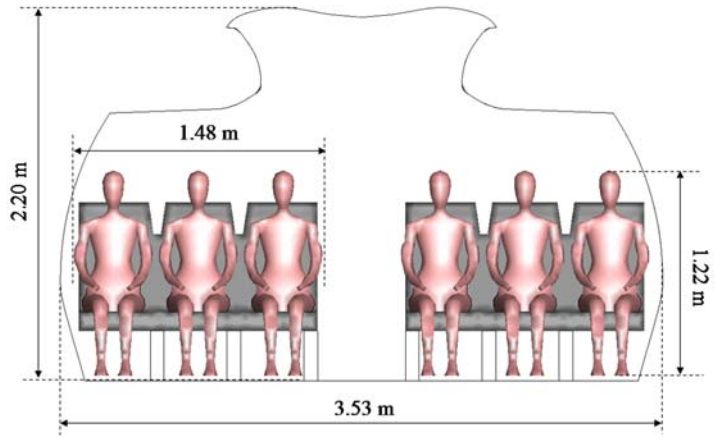

(b)

Figure 2. (a) Schematic of a seven-row section of the fully-occupied economy cabin of a Boeing 737 and (b) Cross-sectional view.

For the Boeing 737 cases, the ventilation rate was set at 0.33 m^3/s for this seven-row section. The supply air velocity from the diffuser ①, ②, ③, and ④ was 2.36, 2.43, 0.91, and 0.57 m/s, respectively. The corresponding Reynolds number was 623, 3206, 2041, and 3008, respectively, with the width of opening as the length scale. The supply air temperature was set at 19.3°C. For the mixing ventilation, the surface temperatures of the cabin side walls, passengers, ceiling, and floor were set at 24.5, 31, 23.8, and 25°C, respectively. For the personalized and conventional displacement systems, the surface temperatures of the ceiling and floor were reversed, since the cold air was supplied from the floor. The turbulence intensity at the diffusers was assumed to be 10%, and the turbulence length scale was set as the width of the opening. Contaminants were released from the breathing zone of the index passenger with a zero initial velocity, which corresponded to a breathing case[54]. The breathing zone was defined as a virtual box of 30 × 30 × 30 cm^3 in front of the mouth[55]. The grid number for the mixing, traditional displacement, and personalized displacement ventilation case was 3.5 million, 3.5 million, and 4.0 million, respectively. The averaged y+ values ranged from 8.2 to 16.2, which were sufficiently fine to correctly predict the convective heat transfer as demonstrated in our previous study[43]. This study employed the SIMPLE algorithm for coupling pressure and velocity, the PRESTO! scheme for discretizing pressure, and the second-order upwind scheme for all the other variables.

In addition to the Boeing 737, this investigation used a twin-aisle Boeing 767 cabin. Figure 3 is a schematic of a seven-row section of the fully-occupied economy cabin of the Boeing 767. The ventilation rate was set at 0.45 m^3/s for the seven-row section. As in the previous aircraft, the mixing ventilation system supplied air through two linear diffusers with a width of 14 mm in the center of the ceiling, ①. Air was extracted through exhaust slots, ②, with a width of 34 mm in the side walls near the floor. The personalized and conventional displacement ventilation systems incorporated two slots in the center of the ceiling, ①, as exhausts. The personalized displacement ventilation system had individual diffusers ③ under the seats, one in front of each passenger, while the conventional displacement ventilation system included two linear diffusers, ②, on the lower side walls. The ventilation rate was set at 0.45 m^3/s for

this seven-row section for all three systems. The supply air velocity from the diffuser ①, ②, and ③ was 2.88, 1.04, and 0.60 m/s, respectively. The corresponding Reynolds number was 2660, 2332, and 3166, respectively. The sources were assumed to be at mouth level of the passengers seated at 4D, 4E, 4F, and 4G. The flight duration was assumed to be five hours. The other setup was the same as that in the Boeing 737 cases. The grid number for the mixing, traditional displacement, and personalized displacement ventilation case was set at 3.3, 3.3, and 4.1 million, respectively. The averaged y+ values ranged from 8.6 to 19.6.

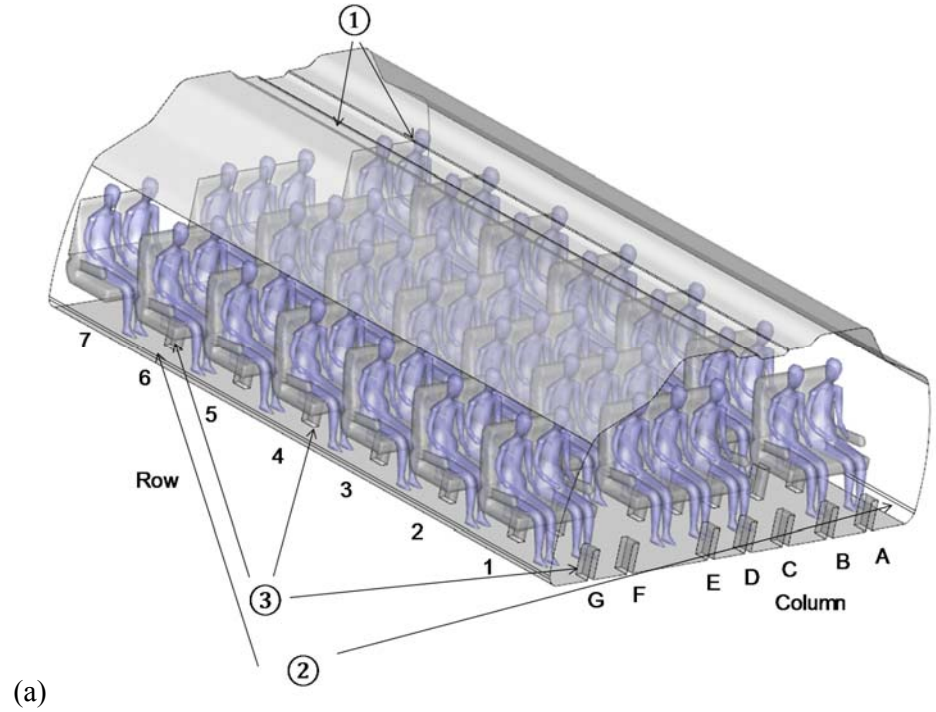

(a)

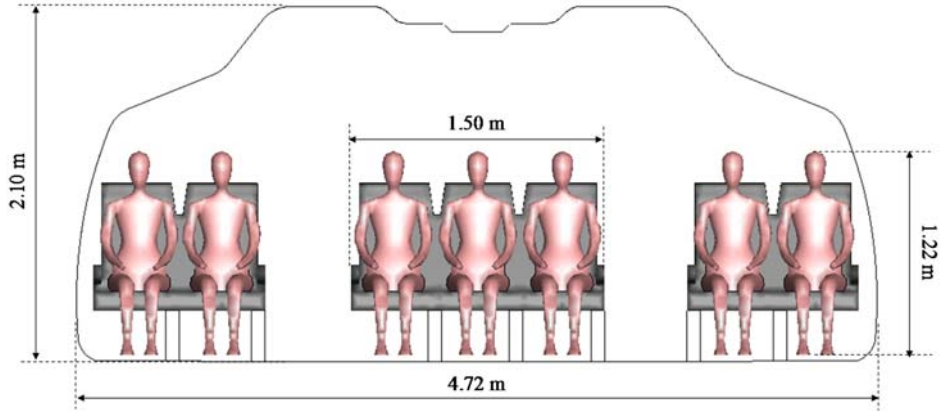

(b)

Figure 3. (a) Schematic of a seven-row section of the fully-occupied, economy cabin of the Boeing 767 and (b) cross-sectional view.

4. Results

4.1 SARS Infection Risk

To evaluate the effectiveness of the three ventilation systems in controlling cabin contaminant transport, this section compares the SARS infection risk distribution in the seven-row section of the cabin mockup when the source is located at different seats.

4.1.1 Boeing 737

Figure 4 displays the cross-sectional air distribution of the Boeing 737 with the mixing ventilation, conventional displacement ventilation, and personalized displacement ventilation systems. The black arrows represent the calculated airflow field. The redlines illustrate the general air structure in the cabins, and indicate the possible paths of the pathogens when exhaled. Since the air distributions were almost symmetric, this sub-section takes the left-hand side of the cabin as an example. In the case of mixing ventilation, the air jet from the diffuser on the upper side of the wall created a large clockwise air circulation. The air from the window seat rose into the upper zone of the aisle and then descended toward the exhaust. For the conventional displacement ventilation, the air from the diffuser in the lower side of the wall first moved horizontally under the seats to the aisle. The air then moved above the seats, travelled to the left, and ascended further to the exhaust in the ceiling. For the personalized displacement ventilation, the air was supplied through the individual diffusers under the seats front of the passengers. Since there were multiple supply air jets, the air distribution above the seats was fairly complex with several small vortices. However, the air pattern above the aisle seat was relatively simple. The upper portion of the air ascended to the exhaust in the ceiling, while the lower portion descended to the zone under the seats. The air distributions shown in Figure 4 will be used in the following sub-sections to interpret the results of the SARS infection risk distributions.

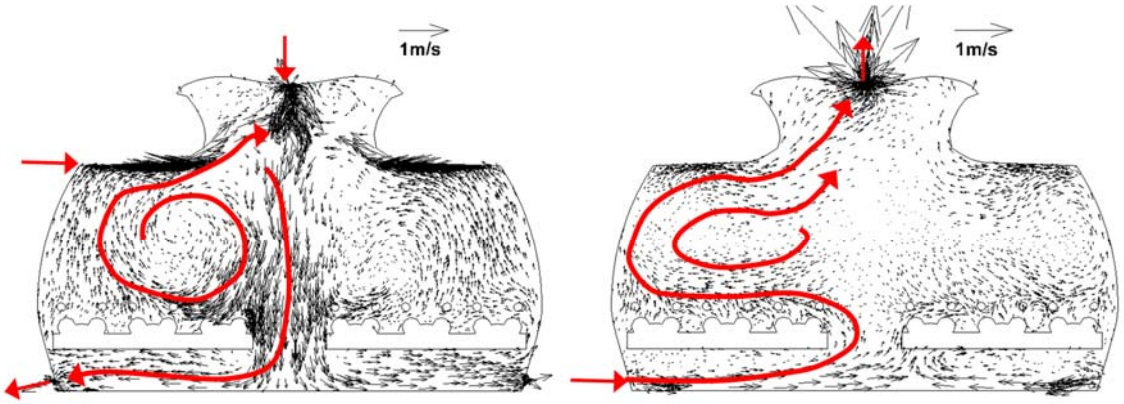

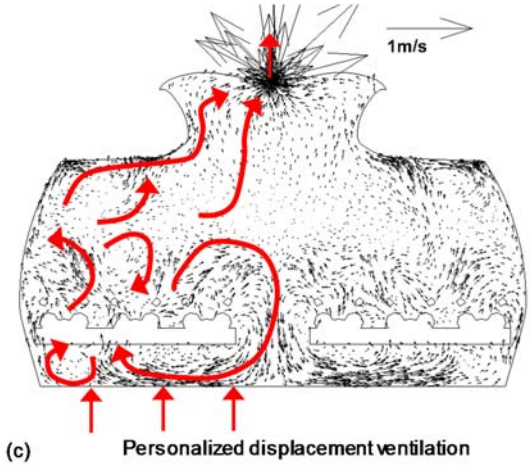

Figure 4. Cross-sectional air distribution in the seven-row section of the Boeing 737 with (a) mixing ventilation, (b) conventional displacement ventilation, and (c) personalized displacement ventilation.

Figure 5 shows the distributions of SARS infection risk with the three different ventilation systems when the index passenger was in seat 4D. In the case of mixing ventilation, the SARS infection risk levels for the passengers in seats 4E and 4F were extremely high (both higher than 0.93). This occurred primarily because the large air circulation transported the exhaled contaminants directly to the window and middle seats. Meanwhile, the two displacement ventilation systems better controlled the infection risks at these two seats. Displacement ventilation was more effective here because the majority of the exhaled contaminants were transported with the upward air directly to the exhaust. Furthermore, for mixing ventilation, a considerable amount of the exhaled contaminants was transported into the aisle and dispersed toward the right-hand side of the cabin. Therefore, the infection risk on the right side of the cabin could be as high as 0.5 for mixing ventilation, whereas that for the two displacement ventilation systems was below 0.3. The average SARS infection risk levels among all the passengers were 0.23, 0.09, and 0.15, respectively, for the mixing ventilation, conventional displacement ventilation, and personalized displacement ventilation systems.

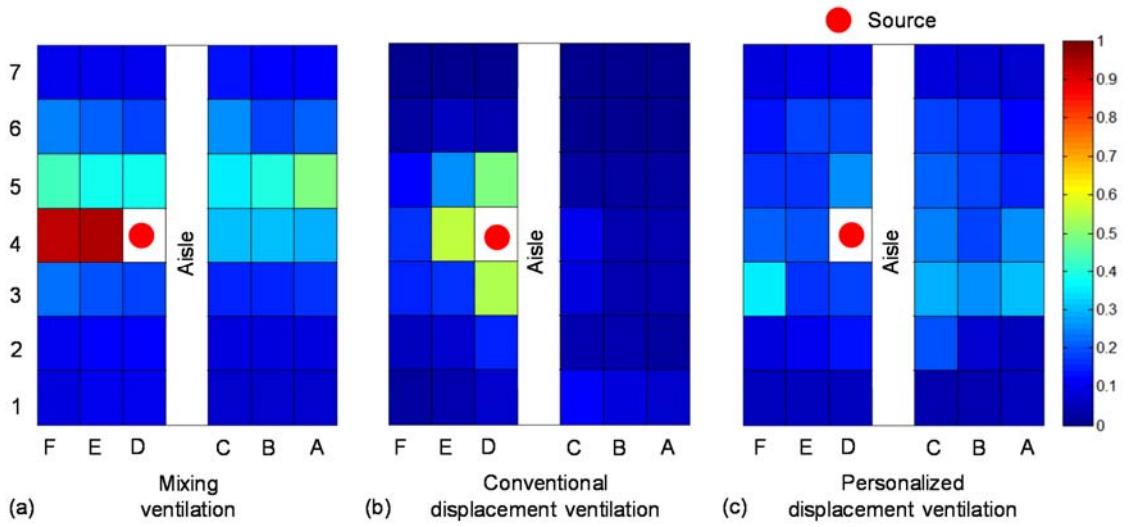

Figure 5. Distributions of SARS infection risk in the seven-row section of the Boeing 737 for a source at aisle seat 4D with (a) mixing ventilation, (b) conventional displacement ventilation, and (c) personalized displacement ventilation.

Figure 6 displays the results when the index passenger was in seat 4E. For mixing ventilation, the SARS infection risk levels for the neighboring passengers in seats 4D and 4F were 0.96 and 0.80, respectively, because of the large clockwise air circulation. For the conventional displacement ventilation, the majority of the exhaled contaminants moved directly toward the exhaust in the ceiling. Thus, the infection risk levels for the neighboring passengers were relatively low. For the personalized displacement ventilation, the source was located in the zone where the air distribution was complex with several small vortices. Contaminant dispersion was caused mainly by turbulence diffusion and was thus less directional. Therefore, the neighboring passengers were exposed to a large amount of the exhaled contaminants. The average SARS infection risk levels among all the passengers were 0.22, 0.07, and 0.14, respectively, for the three ventilation systems.

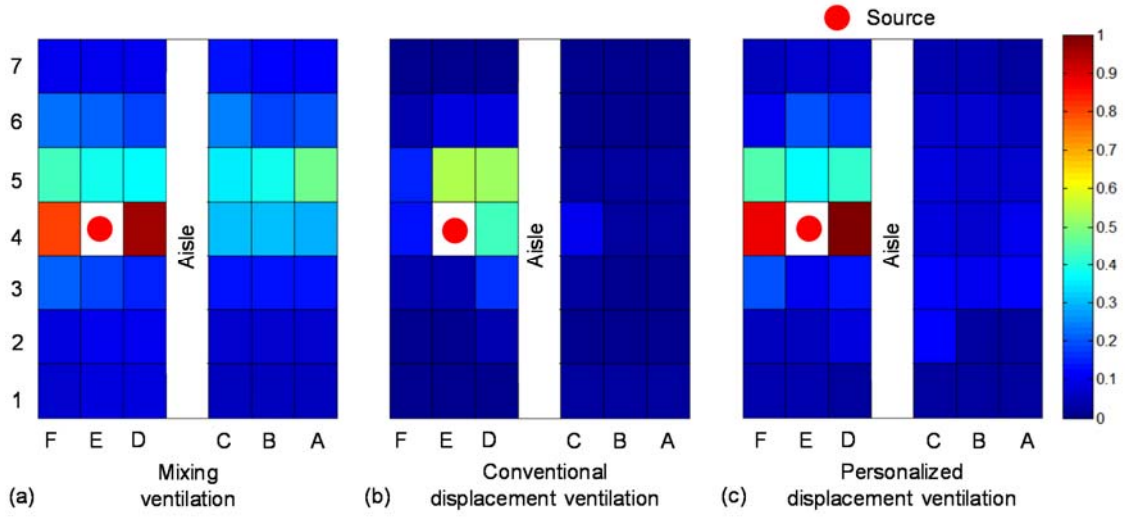

Figure 6. Distributions of SARS infection risk in the seven-row section of the Boeing 737 for a source at middle seat 4E with (a) mixing ventilation, (b) conventional displacement ventilation, and (c) personalized displacement ventilation.

Figure 7 shows the results when the index passenger was in seat 4F. For mixing ventilation, the SARS infection risk levels for the neighboring passengers were much lower than in the previous two cases. This difference occurred because the exhaled contaminants were transported upward along the wall to the aisle, without directly entering the breathing zones of the neighboring passengers. For the conventional displacement ventilation, the neighboring passengers were also at low risk. Interestingly, the passengers in the back seats were at high risk, mainly because of the backward airflow from the breathing zone at seat 4F. For the personalized displacement ventilation, the neighboring passengers were also at high risk. The average SARS infection risk levels among all the passengers were 0.20, 0.12, and 0.12, respectively, for the three systems.

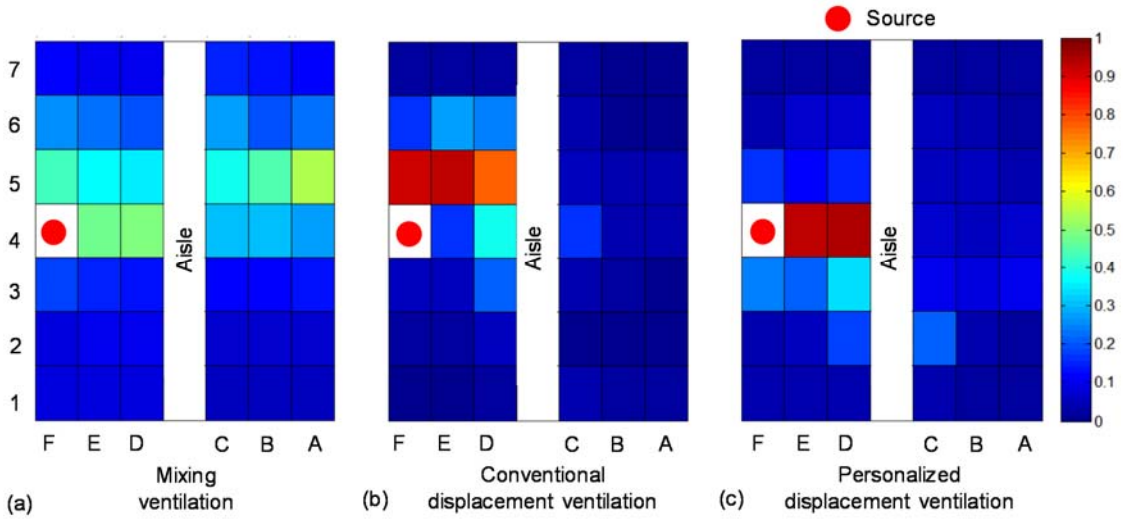

Figure 7. Distributions of SARS infection risk in the seven-row section of the Boeing 737 for a source at window seat 4F with (a) mixing ventilation, (b) conventional displacement ventilation, and (c) personalized displacement ventilation.

In all the above cases, there were 41 (number of passengers with the exception of the source) × 3 (source locations) = 123 data points for SARS infection risk for each ventilation system. This investigation calculated and compared the average SARS infection risk among the 123 data points for the three ventilation systems. As listed in Table 1, compared with the mixing ventilation (0.21), the personalized ventilation (0.14) reduced the overall infection risk by 33% during the two-hour flight. Thus, the number of infected passengers would decrease from 8.6 to 5.7. However, compared with the conventional displacement ventilation (0.09), the personalized displacement ventilation would slightly increase the number of passengers infected with SARS. Therefore, the conventional displacement ventilation system exhibited the best performance, followed by the personalized displacement ventilation system. The mixing ventilation system had the worst performance.

Table 1. Average SARS infection risk in the Boeing 737 for the three ventilation systems.

	Mixing ventilation	Conventional displacement ventilation	Personalized displacement ventilation
Average SARS infection risk	0.21	0.09	0.14

4.1.2 Boeing 767

Figure 8 shows the cross-sectional air distribution in the Boeing 767 aircraft with the three ventilation systems. For mixing ventilation, the air above the middle seats moved upward and then toward the left wall, forming a large counter-clockwise air circulation. Furthermore, there was another relatively small counter-clockwise vortex above the side seats. The conventional displacement ventilation created a more complex air distribution than the mixing ventilation. In general, the air above the middle seats moved to the left side and then travelled upward along the wall to the exhaust in the ceiling. For the personalized displacement ventilation, most of the air above the seats moved upward to the exhaust in the ceiling, but, horizontal air movement still occurred.

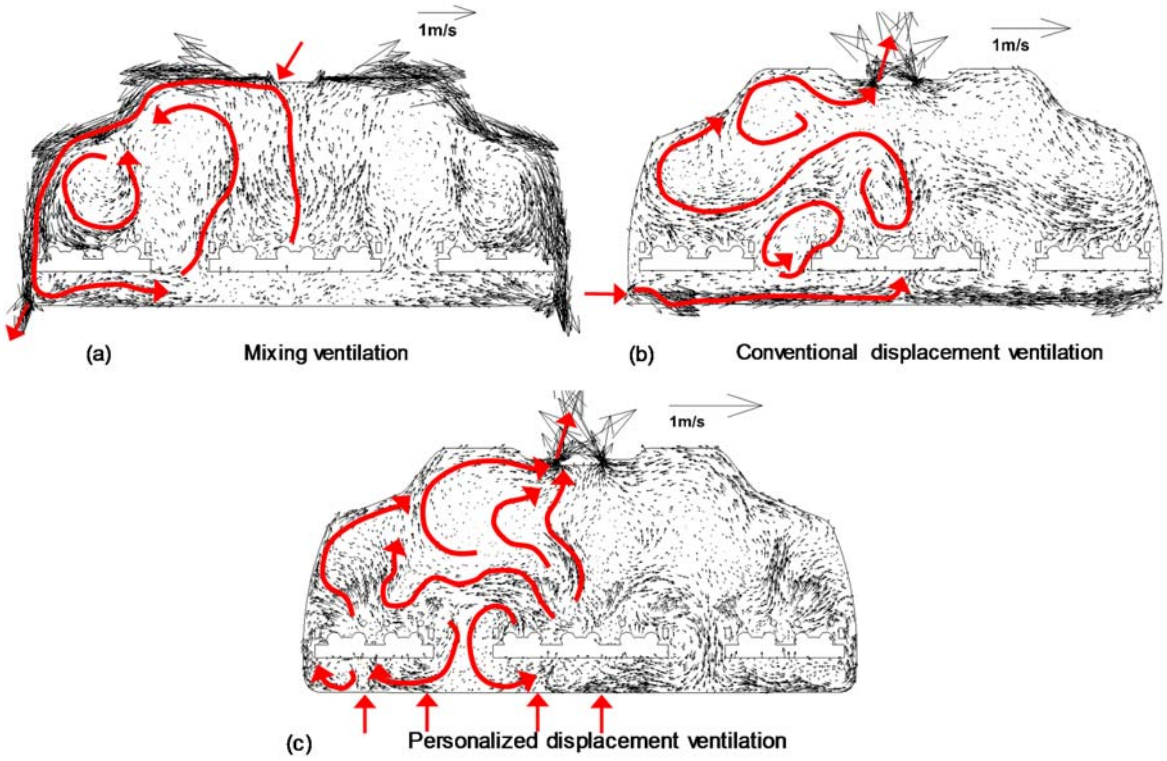

Figure 8. Cross-sectional air distribution in the seven-row section of the Boeing 767 with (a) mixing ventilation, (b) conventional displacement ventilation, and (c) personalized displacement ventilation.

Figures 9 compares the SARS infection risk distribution in the seven-row section of the Boeing 767 with the three ventilation systems when the source was at the middle seat (4D), middle-aisle seat (4E), side-aisle seat (4F), and window seat (4G). The dispersion of the

exhaled contaminants mainly followed the air distribution shown in Figure 8 and resulted in the corresponding infection risk distributions. To keep this paper concise, we have not elaborated here on the detailed contaminant transport patterns for each case. The highest infection risk levels in each case were caused primarily by the movement of air directly from the source to the breathing zone of the particular passenger(s). As in the Boeing 737, the contaminant dispersion under the mixing ventilation was stronger than under the conventional displacement or personalized displacement ventilation. Both the conventional and personalized displacement ventilation systems more effectively limited the influence of exhaled contaminants on the neighboring passengers and the other side of the cabin. As listed in Table 2, the average SARS infection risk levels for the mixing, conventional displacement, and personalized displacement ventilation systems were 0.37, 0.12, and 0.16, respectively. The conclusion for the Boeing 767 aircraft was consistent with that for the Boeing 737.

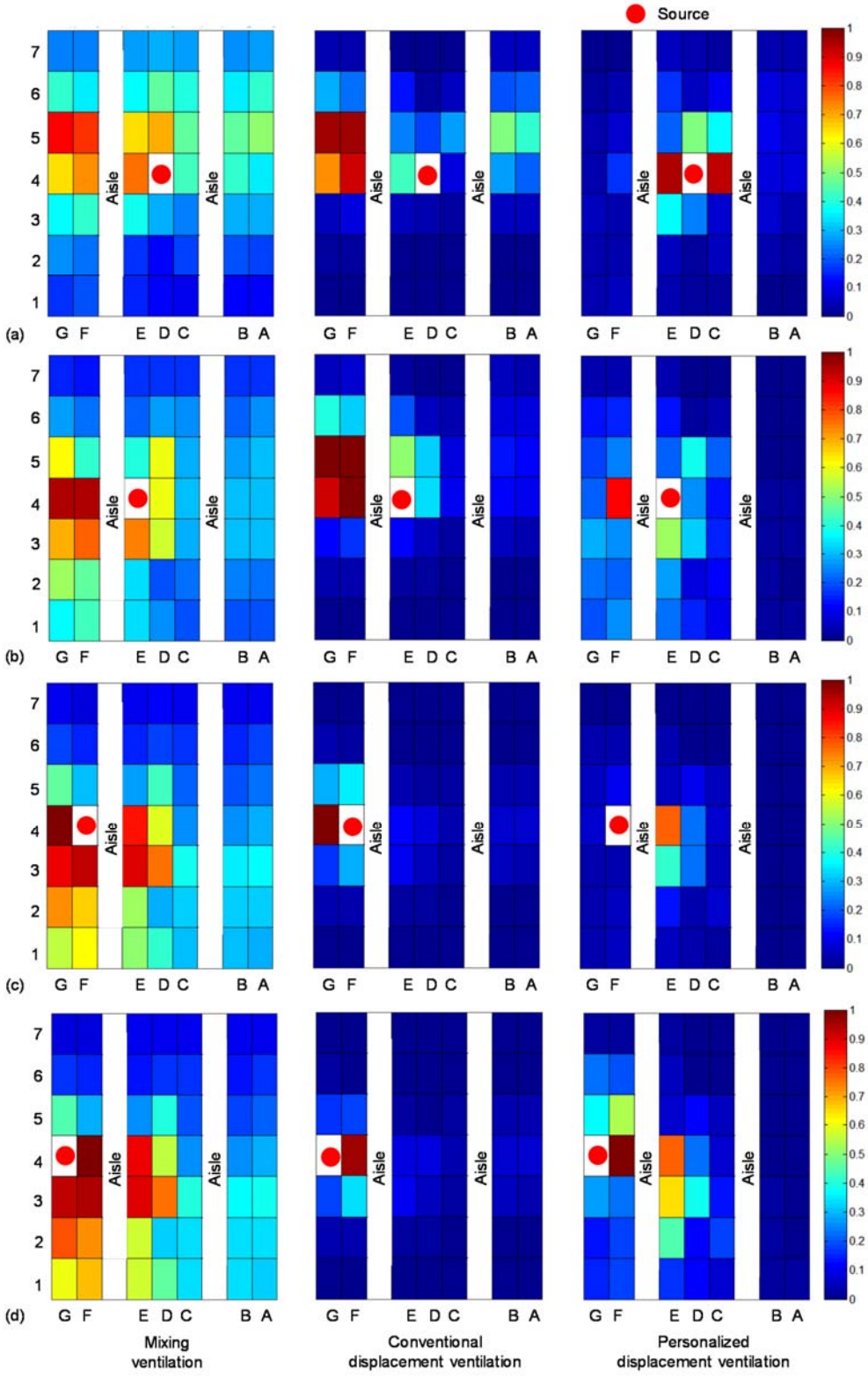

Figure 9. Distributions of SARS infection risk in the seven-row section of the Boeing 767 with the three ventilation systems when the source was at (a) middle seat 4D, (b) middle-aisle seat 4E, (c) side-aisle seat 4F, and (d) window seat 4G.

Table 2. Average SARS infection risk in the Boeing 767 for the three ventilation systems.

	Mixing ventilation	Conventional displacement ventilation	Personalized displacement ventilation
Average SARS infection risk	0.37	0.12	0.16

4.2 Risk of draft

This study calculated the PD distribution on the virtual surface zone 0.1 m away from each passenger for the mixing, conventional displacement, and personalized displacement ventilation systems, as shown in Figure 10. This virtual surface was selected to represent the personal microenvironment as recommended by Liu et al.[26]. Note that only the results for row 4 are shown in the figure, as the PD distributions were similar among different rows. For the mixing ventilation system, the highest PD among the passengers was 32%, was seen at the feet of the passengers in the window seats. This occurred because the passengers' feet were close to the cabin exhausts, and the air velocity near the exhausts was high. For the conventional displacement ventilation system, the highest PD, 43%, was observed in the foot area of the passengers in the window seats. This occurred because the air was supplied in the lower part of the cabin, flowing directly to the feet of the passengers in the window seats. For the personalized displacement ventilation system, the highest PD among the passengers was 31%, in the leg area of the passengers in the middle and aisle seats. This occurred because the individual diffusers near the passengers' feet supplied air obliquely backward, resulting in high air velocity near their legs. From the perspective of highest PD, the performance of the conventional displacement ventilation system was the worst, and the mixing and personalized displacement ventilation systems were comparable.

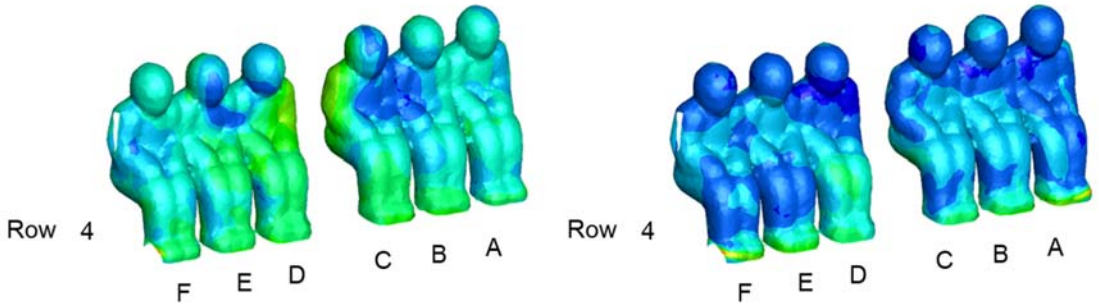

(a) (b)

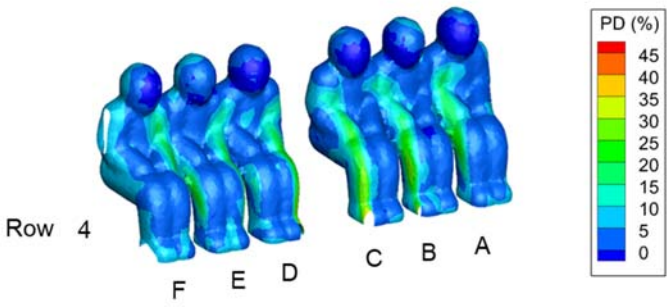

(c)

Figure 10. The PD distributions around the passengers in row 4 in the seven-row section of the Boeing 737 with (a) mixing ventilation, (b) conventional displacement ventilation, and (c) the personalized displacement ventilation system.

Note that the PD distribution was not necessarily uniform on the virtual surface for a particular passenger. In other words, a passenger might feel discomfort due to the draft only at certain areas of the body, such as the feet or shoulders. According to the ASHRAE standards, PD greater than 15% is considered discomfort. Therefore, this study further calculated the percentage of the area on the virtual surface with PD greater than 15%, $P_{discomfort}$, for each passenger by:

$$P_{discomfort} = \frac{A(PD > 15\%)}{A_{virtual\_total}} \times 100\% \quad (4)$$

where A(PD > 15%) is the area on the virtual surface with PD greater than 15% and $A_{virtual\_total}$ is the total area of the virtual surface 0.1 m away from the passenger.

For the mixing ventilation system, the average $P_{discomfort}$ among all the passengers was 10.1%. The draft was due to the large vortex that formed on each side of the cabin in the occupied zone[56]. For the conventional displacement system, the average $P_{discomfort}$ was clearly smaller, only 6.5%. The reason for the difference was that the air velocities were relatively low, as shown in Figure 4. For the personalized displacement system, the average $P_{discomfort}$ was 5.4%, the lowest among the systems. From the perspective of average $P_{discomfort}$, the personalized displacement ventilation system had the best performance, while the worst case was the mixing ventilation system. In summary, when both the highest PD and the average $P_{discomfort}$ are taken into consideration, the personalized displacement ventilation system provided the best thermal comfort among the three systems.

Figure 11 shows the results for the Boeing 767. The highest PD values among passengers in the cabin with the mixing, conventional displacement, and personalized displacement ventilation system were 29%, 39%, and 28%, respectively, which were similar to the results for the Boeing 737. In addition, the average $P_{discomfort}$ among passengers in the cabin with the mixing ventilation system (12.3%) was significantly larger than with the other two systems.

The average $P_{discomfort}$ values were 9.8% and 5.4%, respectively, for the conventional and the personalized displacement ventilation systems. Therefore, for both aircraft, the personalized ventilation system provided the highest level of thermal comfort in the cabin, while the mixing ventilation system provided the lowest comfort level.

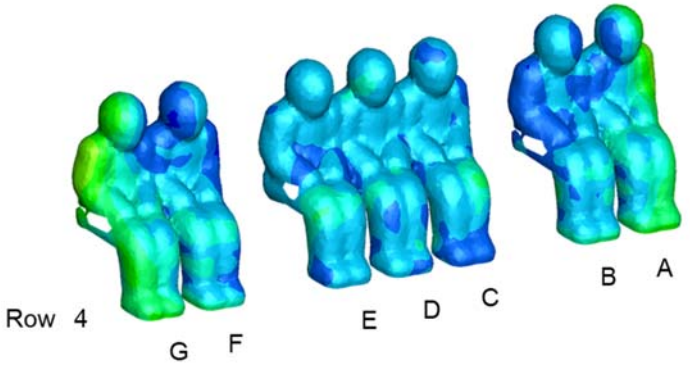

(a)

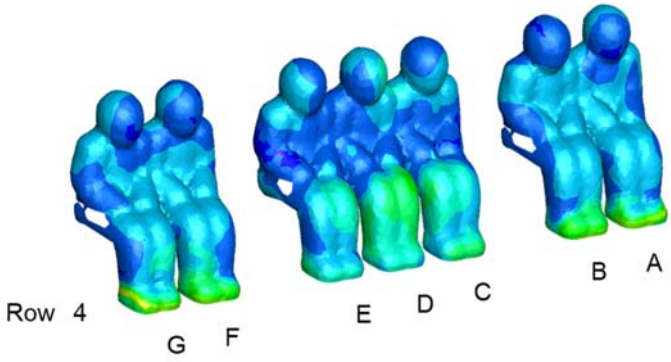

(b)

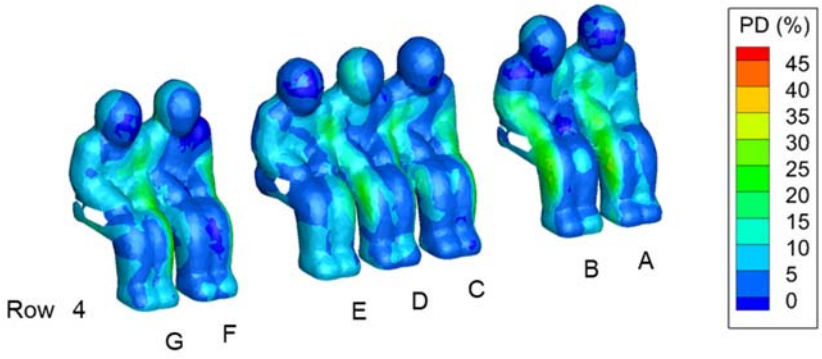

(c)

Figure 11. The PD distributions around the passengers in row 4 in the seven-row section of the Boeing 767 with (a) the mixing ventilation system, (b) the conventional displacement ventilation systems, and (c) the personalized displacement ventilation system.

5. Discussion

This study employed the Wells-Riley method to evaluate the SARS infection risk. Dose-response models are more biologically plausible, since they are based on experimental infectious dose data[57]. However, apart from indirect studies[58] on infectivity of SRAS viruses, direct infectious dose data is not available for SARS because of its lethality. Moreover, this investigation aimed to compare the performance of three different air distribution systems. The Wells-Riley method provided a quick and simple assessment within the scope of the study. Other diseases could be investigated using dose-response models in future studies.

Supply air distribution was assumed to be uniform, and a standard manikin was used to represent passengers. The airflow boundary conditions would be very complex in a real, operating airplane cabin[59], and passengers could have different body sizes, poses, and metabolic rates. Thus, there may be discrepancies between the CFD results and real-life conditions. The purpose of this study was to design and evaluate the cabin environment, and the use of design conditions was adequate.

There are several future research directions. First, Although the transmission of SARS viruses was proven to be airborne in or between buildings[60], the airborne transmission of SARS in aircraft cabins is an assumption. For instance, Lei et al.[61] suggested that the fomite might also be responsible for the transmission of SARS. Even for other infectious diseases, the transmission can also occur through indirect contact. For example, the surfaces in the cabin can become contaminated by the deposition of airborne pathogens or physical touch by the index passenger[62]. If other passengers touched the contaminated surfaces[62], or the deposited pathogens resuspended in the air[63] and were inhaled by the other passengers, infections could also occur. These transmission routes and mechanisms in the cabin merit further investigation. Furthermore, this study assumed that all the gaspers were turned off. In practice, passengers may turn on the gaspers for individual thermal regulation. According to one of our previous studies, gasper-induced airflow has mixed effects on cabin air quality in airplanes with mixing ventilation[38]. The ways in which gaspers might influence the transmission of airborne infectious diseases in aircraft cabins with conventional and personalized ventilation are still unclear. The impact of gaspers deserves in-depth exploration in future studies. In addition, it is possible to develop a hybrid system which combines both the personalized displacement air diffusers and the overhead mixing diffusers in order to reduce the draft risk near the legs by supplying smaller amount of local air. This type of hybrid system also requires detailed airflow and contaminant transport analysis using the proposed approach.

6. Conclusions

This investigation aimed to evaluate the effectiveness of three different ventilation systems in controlling contaminant transport and maintaining cabin thermal comfort. This study first used the Wells-Riley equation integrated with CFD to obtain the SARS quanta value based on a SARS outbreak on a flight from Hong Kong to Beijing during the 2003 SARS epidemic. The investigation then assessed the performance of the three systems in a seven-row section of the fully occupied, economy-class cabin of a Boeing 737 airplane and a Boeing 767. Within the scope of this study, the following conclusions can be made:

(1) For all the assumed source locations in both airplanes, the passengers' infection risk by air was the highest with the mixing ventilation system. The conventional displacement ventilation system produced the lowest infection risk.
(2) The personalized ventilation system performed the best in maintaining thermal comfort in the cabin and can also reduce the infection risk by air. This system is recommended for airplane cabins.

References

1. Moser MR, Bender TR, Margolis HS, Noble GR, Kendal AP, Ritter DG. An outbreak of influenza aboard a commercial airliner. *Am J Epidemiol*. 1979; 110:1-6.

2. Kenyon TA, Valway SE, Ihle WW, Onorato IM, Castro KG. Transmission of multidrug-resistant Mycobacterium tuberculosis during a long airplane flight. *N Engl J Med*. 1996; 334:933-938.

3. Olsen SJ, Chang HL, Cheung TYY, Tang AFY, Fisk TL, Ooi SPL, Kuo HW, Jiang DDS, Chen KT, Lando J, Hsu KH. Transmission of the severe acute respiratory syndrome on aircraft. *N Engl J Med*. 2003; 349:2416-2422.

4. ACI (Airports Council International). The Global Airport Community. 2007. http://www.airports.org/aci/aci/file/AnnualReport/ACIAnnualReport2006FINAL.pdf.

5. Li Y, Leung GM, Tang JW, Yang X, Chao CYH, Lin JZ, Lu JW, Nielsen PV, Niu J, Qian H, Sleigh AC. Role of ventilation in airborne transmission of infectious agents in the built environment–A multidisciplinary systematic review. *Indoor Air*. 2007; 17:2-18.

6. Liu W, Mazumdar S, Zhang Z, Poussou SB, Liu J, Lin CH, Chen Q. State-of-the-art methods for studying air distributions in commercial airliner cabins. *Build Environ*. 2012; 47:5-12.

7. Schuchardt S, Koch W, Rosenberger W. Cabin air quality–Quantitative comparison of volatile air contaminants at different flight phases during 177 commercial flights. *Build Environ*. 2019; 148:498-507.

8. Fišer J and Jícha M. Impact of air distribution system on quality of ventilation in small aircraft cabin. *Build Environ*. 2013; 69:171-182.

9. Wu Y, Liu H, Li B, Cheng Y, Tan D, Fang Z. Thermal comfort criteria for personal air supply in aircraft cabins in winter. *Build Environ*. 2017; 125:373-382.

10. Maier J, Marggraf-Micheel C, Dehne T, Bosbach J. Thermal comfort of different displacement ventilation systems in an aircraft passenger cabin. *Build Environ*. 2017; 111:256-264.

11. Maier J, Marggraf-Micheel C, Zinn F, Dehne T, Bosbach J. Ceiling-based cabin displacement ventilation in an aircraft passenger cabin: Analysis of thermal comfort. *Build Environ*. 2018; 146:29-36.

12. Cui W, Ouyang Q, Zhu Y. Field study of thermal environment spatial distribution and passenger local thermal comfort in aircraft cabin. *Build Environ*. 2014; 80:213-220.

13. Cao X, Li J, Liu J, Yang W. 2D-PIV measurement of isothermal air jets from a multi-slot diffuser in aircraft cabin environment. *Build Environ*. 2016; 99:44-58.

14. Wang C, Liu J, Li J, Guo Y, Jiang N. Turbulence characterization of instantaneous airflow in an aisle of an aircraft cabin mockup. *Build Environ*. 2017; 116:207-217.

15. Li J, Liu J, Wang C, Wesseling M, Müller D. PIV experimental study of the large-scale dynamic airflow structures in an aircraft cabin: Swing and oscillation. *Build Environ*. 2017; 125:180-191.

16. Li J, Cao X, Liu J, Wang C, Zhang Y. Global airflow field distribution in a cabin mock-up measured via large-scale 2D-PIV. *Build Environ*. 2015; 93:234-244.

17. Zhang Y, Liu J, Pei J, Wang C. Statistical analysis of turbulent thermal convection in a cabin mockup. *Build Environ*. 2017; 115:34-41.

18. Tang Z, Cui X, Guo Y, Jiang N, Dai S, Liu J. Near fields of gasper jet flows with wedged nozzle in aircraft cabin environment. *Build Environ*. 2017; 125:99-110.

19. Li J, Liu J, Dai S, Guo Y, Jiang N, Yang W. PIV experimental research on gasper jets interacting with the main ventilation in an aircraft cabin. *Build Environ*. 2018; 138:149-159.

20. Dai S, Sun H, Liu W, Guo Y, Jiang N, Liu J. Experimental study on characteristics of the jet flow from an aircraft gasper. *Build Environ*. 2015; 93:278-284.

21. Guo Y, Jiang N, Yao S, Dai S, Liu J. Turbulence measurements of a personal airflow outlet jet in aircraft cabin. *Build Environ*. 2014; 82:608-617.

22. Zhang Z, Chen X, Mazumdar S, Zhang T, Chen Q. Experimental and numerical investigation of airflow and contaminant transport in an airliner cabin mockup. *Build Environ*. 2009; 44:85-94.

23. Li B, Duan R, Li J, Huang Y, Yin H, Lin CH, Wei D, Shen X, Liu J, Chen Q. Experimental studies of thermal environment and contaminant transport in a commercial aircraft cabin with gaspers on. *Indoor Air*. 2016; 26:806-819.

24. Pang L, Li P, Bai L, Liu D, Zhou Y, Yao J. Optimization of air distribution mode coupled interior design for civil aircraft cabin. *Build Environ*. 2018; 134:131-145.

25. Zhao X, Liu W, Lai D, Chen Q. Optimal design of an indoor environment by the CFD-based adjoint method with area-constrained topology and cluster analysis. *Build Environ*. 2018; 138:171-180.

26. Liu W, Duan R, Chen C, Lin CH, Chen Q. Inverse design of the thermal environment in an airliner cabin by use of the CFD-based adjoint method. *Energy Build.* 2015; 104: 147-155.

27. Zhang TH and You XY. A simulation-based inverse design of preset aircraft cabin environment. *Build Environ*. 2014; 82:20-26.

28. Wei Y, Zhang TT, Wang S. Prompt design of the air-supply opening size for a commercial airplane based on the proper orthogonal decomposition of flows. *Build Environ*. 2016; 96:131-141.

29. Chen C, Liu W, Li F, Lin CH, Liu J, Pei J, Chen Q. A hybrid model for investigating transient particle transport in enclosed environments. *Build Environ*. 2013; 62:45-54.

30. Chen C, Lin CH, Long Z, Chen Q. Predicting transient particle transport in enclosed environments with the combined computational fluid dynamics and Markov chain method. *Indoor Air.* 2014; 24:81-92.

31. Chen C, Liu W, Lin CH, Chen Q. Comparing the Markov chain model with the Eulerian and Lagrangian models for indoor transient particle transport simulations. *Aerosol Sci Technol.* 2015; 49:857-871.

32. Qian H, Li Y, Nielsen P and Huang X. Spatial distribution of infection risk of SARS transmission in a hospital ward. *Build. Environ*. 2009; 44: 1651-1658.33. Yan Y, Li X, Shang Y, Tu J. Evaluation of airborne disease infection risks in an airliner cabin using the Lagrangian-based Wells-Riley approach. *Build Environ*. 2017; 121:79-92.

34. Gupta JK, Lin CH, Chen Q. Risk assessment of airborne infectious diseases in aircraft cabins. *Indoor Air.* 2012; 22:388-395.

35. Wei Y, Zhou H, Zhang TT, Wang S. Inverse identification of multiple temporal sources releasing the same tracer gaseous pollutant. *Build Environ*. 2017; 118:184-195.

36. Wang H, Lu S, Cheng J, Zhai ZJ. Inverse modeling of indoor instantaneous airborne contaminant source location with adjoint probability-based method under dynamic airflow field. *Build Environ*. 2017; 117:178-190.

37. Zhang T and Chen QY. Novel air distribution systems for commercial aircraft cabins. *Build Environ*. 2007; 42:1675-1684.

38. You R, Liu W, Chen J, Lin CH, Wei D, Chen Q. Predicting airflow distribution and contaminant transport in aircraft cabins with a simplified gasper model. *J Build Perform Simul.* 2016; 9:699-708.

39. You R, Chen J, Lin CH, Wei D, Chen Q. Investigating the impact of gaspers on cabin air quality in commercial airliners with a hybrid turbulence model. *Build Environ*. 2017; 111:110-122.

40. Bosbach J, Heider A, Dehne T, Markwart M, Gores I, Bendfeldt P. Evaluation of cabin displacement ventilation under flight conditions. 28th Congress of the International Council of the Aeronautical Sciences; September 23-28, 2012; Brisbane, Australia. http://www.icas.org/ICAS_ARCHIVE/ICAS2012/PAPERS/304.PDF

41. Schmidt M, Müller D, Gores I, Markwart M. Numerical study of different air distribution systems for aircraft cabins. 11th International Conference on Indoor Air Quality and Climate; August 17-22, 2008; Copenhagen, Denmark.

42. Müller D, Schmidt M, Müller D. Application of a displacement ventilation system for air distribution in aircraft cabins. Proceedings of the 3rd International Workshop on Aviation System Technology; March 31-April 1, 2011; Hamburg, Germany.

43. You R, Zhang Y, Zhao X, Lin CH, Wei D, Liu J, Chen Q. An innovative personalized displacement ventilation system for airliner cabins. *Build Environ*. 2018; 137:41-50.

44. You R, Chen J, Shi Z, Liu W, Lin CH, Wei D, Chen Q. Experimental and numerical study of airflow distribution in an aircraft cabin mock-up with a gasper on. *J Build Perform Simul.* 2016; 9:555-566.

45. Chen Q. Comparison of different k-ε models for indoor air flow computations. *Numer Heat Tr B-Fund*. 1995; 28:353-369.

46. Zhang Z, Zhang W, Zhai ZJ, Chen QY. Evaluation of various turbulence models in predicting airflow and turbulence in enclosed environments by CFD: Part 2—Comparison with experimental data from literature. *HVAC&R Res.* 2007; 13:871-886.

47. Wang M and Chen Q. Assessment of various turbulence models for transitional flows in an enclosed environment (RP-1271). *HVAC&R Res.* 2009; 15:1099-1119.

48. Zhang Z and Chen Q. Comparison of the Eulerian and Lagrangian methods for predicting particle transport in enclosed spaces. *Atmos environ.* 2007; 41:5236-5248.

49. ANSYS. *Fluent 12.1 Documentation*. Lebanon, NH: Fluent Inc.; 2010.

50. Hinds, William C. *Aerosol technology: properties, behavior, and measurement of airborne particles*. John Wiley & Sons, 2012.

51. ISO. Respiratory Protective Devices—Human Factors. Part 1. Metabolic Rates and Respiratory Flow Rates. Geneva, ISO/TS, 16976–1, 2007.

52. Fanger PO, Melikov AK, Hanzawa H, Ring J. Air turbulence and sensation of draught. *Energy Build.* 1988; 12:21-39.53. ASHRAE. Air Quality within Commercial Aircraft. In *ASHRAE Standard 161-2007*. American Society of Heating, Refrigerating and Air-Conditioning Engineers; 2007.

54. Chen C, Lin C-H, Jiang Z, Chen Q. Simplified models for exhaled airflow from a cough with the mouth covered. *Indoor Air*. 2014: 24, 580-591.

55. Occupational Safety & Health Administration (OSHA). OSHA Technical Manual (OTM). Section II: Chapter 1, Personal sampling for air contaminants. 2014. Available: https://www.osha.gov/dts/osta/otm/otm_ii/pdfs/otmii_chpt1_allinone.pdf

56. Cui W and Zhu Y. Systematic study on passengers' thermal comfort under low-air-pressure environment in commercial aircraft cabin. In Annual Meeting of the Center for Cabin Air Reformative Environment; 2015; Chongqing, China.

57. Sze To GN and Chao CYH. Review and comparison between the Wells-Riley and dose-response approaches to risk assessment of infectious respiratory diseases. *Indoor Air.* 2010; 20:2-16.

58. Xiao S, Li Y, Wong T-W, Hui DSC. Role of fomites in SARS transmission during the largest hospital outbreak in Hong Kong. *Plos One*. 2017: 12(7): e0181558.

59. Liu W, Wen J, Chao J, Yin W, Shen C. Lai D, Lin CH, Liu J, Sun H, Chen Q. Accurate and high-resolution boundary conditions and flow fields in the first-class cabin of an MD-82 commercial airliner. *Atmos Environ.* 2012; 56:33-44.

60. Yu ITS, Li Y, Wong TW, Tam W, Chan A, Lee JHW, Leung DYC, Ho T. Evidence of airborne transmission of the severe acute respiratory syndrome virus. *N Engl J Med*. 2004: 350, 1731-1739.

61. Lei H, Li Y, Xiao S, Lin CH, Norris SL, Wei D, Hu Z, Ji S. Routes of transmission of influenza A H1N1, SARS CoV, and norovirus in air cabin: Comparative analyses. *Indoor Air*. 2018; 28(3), 394-403.

62. Zhang N, Li Y, Huang H. Surface touch and its network growth in a graduate student office. *Indoor Air.* 2018; 28:963-972.

63. Zhang N and Li Y. Transmission of Influenza A in a student office based on realistic person-to-person contact and surface touch behaviour. *Int J Environ Res Public Health.* 2018; 15:1699.